A&A 487, 7–17 (2008)
DOI: 10.1051/0004-6361:20078891

Astronomy & Astrophysics

The VIMOS VLT Deep Survey

Testing the gravitational instability paradigm at $z \sim 1$

C. Marinoni[1], L. Guzzo[2,3], A. Cappi[4], O. Le Fèvre[5], A. Mazure[5], B. Meneux[3], A. Pollo[6], A. Iovino[2], H. J. McCracken[7], R. Scaramella[8], S. de la Torre[5], J. M. Virey[1], D. Bottini[9], B. Garilli[9], V. Le Brun[5], D. Maccagni[9], J. P. Picat[10], M. Scodeggio[9], L. Tresse[5], G. Vettolani[11], A. Zanichelli[11], C. Adami[5], S. Arnouts[5], S. Bardelli[4], M. Bolzonella[4], S. Charlot[7], P. Ciliegi[11], T. Contini[10], S. Foucaud[12], P. Franzetti[9], I. Gavignaud[13], O. Ilbert[14], F. Lamareille[10], B. Marano[15], G. Mathez[10], R. Merighi[4], S. Paltani[16,17], R. Pellò[10], L. Pozzetti[4], M. Radovich[18], D. Vergani[9], G. Zamorani[4], E. Zucca[4], U. Abbas[5], M. Bondi[11], A. Bongiorno[11], J. Brinchmann[19], A. Buzzi[1], O. Cucciati[5,20], L. de Ravel[5], L. Gregorini[11], Y. Mellier[7], P. Merluzzi[18], E. Perez-Montero[10], P. Taxil[1], S. Temporin[5], and C. J. Walcher[7]

[1] Centre de Physique Théorique, UMR 6207 CNRS-Université de Provence, Case 907, 13288 Marseille, France
e-mail: marinoni@cpt.univ-mrs.fr
[2] INAF – Osservatorio Astronomico di Brera, via Brera 28, 20121 Milano, Italy
[3] Max Planck Institut für extraterrestrische Physik, 85741 Garching, Germany
[4] INAF – Osservatorio Astronomico di Bologna, via Ranzani 1, 40127 Bologna, Italy
[5] Laboratoire d'Astrophysique de Marseille, UMR 6110, BP8 Traverse du Siphon, 13012 Marseille, France
[6] Astronomical Observatory of the Jagiellonian University, ul Orla 171, 30-244 Krakow, Poland
[7] Institut d'Astrophysique de Paris, UMR 7095, 98 bis Bvd. Arago, 75014 Paris, France
[8] INAF – Osservatorio Astronomico di Roma, via Osservatorio 2, 00040 Monteporzio Catone (Roma), Italy
[9] INAF – IASF, via Bassini 15, 20133 Milano, Italy
[10] LAT – Observatoire Midi-Pyrénées, UMR5572, 14 av. E. Belin, 31400 Toulouse, France
[11] INAF – Istituto di Radio-Astronomia, via Gobetti 101, 40129 Bologna, Italy
[12] School of Physics & Astronomy, University of Nottingham, University Park, Nottingham, NG72RD, UK
[13] Astrophysical Institute Potsdam, An der Sternwarte 16, 14482, Potsdam, Germany
[14] Institute for Astronomy, 2680 Woodlawn Dr., University of Hawaii, Honolulu, Hawaii, 96822, USA
[15] Università di Bologna, Dipartimento di Astronomia, via Ranzani 1, 40127 Bologna, Italy
[16] Integral Science Data Centre, ch. d'Écogia 16, 1290, Versoix, Switzerland
[17] Geneva Observatory, ch. des Maillettes 51, 1290, Sauverny, Switzerland
[18] INAF – Osservatorio Astronomico di Capodimonte, via Moiariello 16, 80131 Napoli, Italy
[19] Centro de Astrofísica da Universidade do Porto, Rua das Estrelas, 4150-762, Porto, Portugal
[20] Università di Milano-Bicocca, Dipartimento di Fisica, Piazza della scienza 3, 20126 Milano, Italy

Received 22 October 2007 / Accepted 12 January 2008

ABSTRACT

We have reconstructed the three-dimensional density fluctuation maps to $z \sim 1.5$ using the distribution of galaxies observed in the VVDS-Deep survey. We use this overdensity field to measure the evolution of the probability distribution function and its lower-order moments over the redshift interval $0.7 < z < 1.5$. We apply a self-consistent reconstruction scheme which includes a complete non-linear description of galaxy biasing and which has been thoroughly tested on realistic mock samples. We find that the variance and skewness of the galaxy distribution evolve over this redshift interval in a way that is remarkably consistent with predictions of first- and second-order perturbation theory. This finding confirms the standard gravitational instability paradigm over nearly 9 Gyr of cosmic time and demonstrates the importance of accounting for the non-linear component of galaxy biasing to consistently reproduce the higher-order moments of the galaxy distribution and their evolution.

Key words. cosmology: large-scale structure of Universe – cosmology: theory – galaxies: statistics – galaxies: high-redshift – Galaxy: evolution

1. Introduction

According to Thomas Wright mapping the Cosmos on the very largest scales is about gaining *"a partial View of Immensity, or without much Impropriety perhaps, a finite View of Infinity"*[1]. Unfortunately, charting the cosmic territory beyond our local volume into the distant Universe is observationally challenging. Until recently, our understanding of the large-scale organisation of galaxies at $z \gtrsim 0.2$ had to rely on the predictions of numerical simulations in the framework of the rather successful cold dark matter model (e.g. Springel et al. 2005).

Within this scenario, which has now developed into the leading theoretical paradigm for the formation of structures in the Universe, structures grow from weak, dark-matter density

[1] *An Original Theory of the Universe* (1750, 9th letter, Plate XXXI).

fluctuations present in the otherwise homogeneous and rapidly expanding early universe. The standard version of the model incorporates the assumption that this primordial, Gaussian-distributed fluctuations are amplified by gravity, eventually turning into the rich structures we see today.

This picture in which gravity, as described by general relativity, is the engine driving cosmic growth is generally referred to as the gravitational instability paradigm (GIP). However plausible it may seem, it is important to test its validity. In the local universe the GIP paradigm has been shown to make sense of a vast amount of independent observations on different spatial scales from galaxies to superclusters of galaxies (e.g. Peacock et al. 2001; Tegmark et al. 2006). Deep redshift surveys now allow us to test whether the predictions of this assumption are also valid at earlier epochs.

In this paper we test the role of gravity in shaping density inhomogeneities by using three-dimensional maps of the distribution of visible matter revealed by the VIMOS-VLT Deep Survey over the large redshift baseline $0 < z < 1.5$ (see Massey et al. 2007, for three dimensional cartography of mass overdensities in the COSMOS field). We present first a qualitative picture of the large-scale organization of remote cosmic structures, and then quantify the observed clustering by computing the probability distribution functions (PDF) of galaxy overdensities δ_g. In this way, we trace how the amplitude and spatial arrangement of galaxy fluctuations changes with cosmic time. We explore the mechanisms governing this growth by comparing the time evolution of the low-order moments of the galaxy PDF, (i.e. the *variance* amplitude $\langle\delta_g^2\rangle$ and the *normalised skewness* $S_3 = \langle\delta_g^3\rangle_c/\langle\delta_g^2\rangle^2$) with the corresponding quantity theoretically predicted for matter fluctuations in the linear and semi-linear perturbative regime. (Note that in the following we shall often speak equivalently of the variance or of its square root, i.e. the *root mean square* amplitude $\langle\delta_g^2\rangle^{1/2}$ when referring to the second-order moment). This provides a test of GIP-specific predictions at as-yet unexplored epochs that are intermediate between the present era and the time of decoupling. Knowledge of the precise growth history of density inhomogeneities provides also a way to test the theory of gravitation (e.g. Linder 2005).

In addition to the statistical approach presented in this paper, we have recently addressed this same issue also from a dynamical point of view. We have used linear redshift-space distortions in the VVDS-*Wide* data to measure the growth rate of matter fluctuations at $z \sim 0.8$ (Guzzo et al. 2008). This approach offers promising prospects for determining the cause of cosmic acceleration in the near future (Linder 2007). The work presented here is also complemented by a parallel paper (Cappi et al. 2008) in which we study the behavior of the N-point correlation functions for this same sample. Higher-order galaxy correlation functions are known to display a hierarchical scaling as a function of the variance of the count distribution (e.g. Peebles 1980). In the same spirit, we use this scaling to test the standard assumption of evolution under gravitational instability of an initially Gaussian distribution of density fluctuations.

The paper is organised as follows: in Sect. 2 we briefly describe the first-epoch VVDS data sample. In Sect. 3 we present 3D overdensity maps from the galaxy distribution in the VVDS to $z \sim 1.5$; we then characterise the evolution of galaxy fluctuations with cosmic epoch by computing their PDF in two redshift slices. In Sect. 4 we compare the observed redshift evolution of the low-order moments (i.e. variance and skewness) of the PDF of the galaxy fluctuations with linear and semi-linear theoretical predictions of the Gravitational Instability Paradigm. Conclusions are presented in Sect. 5.

The coherent cosmological picture emerging from independent observations and analysis motivates us to present our results in the context of a ΛCDM cosmological model with $\Omega_m = 0.3$ and $\Omega_\Lambda = 0.7$. Throughout, the Hubble constant is parameterised via $h = H_0/100$. All magnitudes in this paper are in the AB system (Oke & Gunn 1983), and from now on we will drop the suffix AB.

2. The first-epoch VVDS-Deep redshift sample

The primary observational goal of the VIMOS-VLT Redshift Survey as well as the survey strategy and first-epoch observations in the VVDS-0226-04 field (from now on simply VVDS-02h) are presented by Le Fèvre et al. (2005). Here it is enough to stress that, in order to minimise selection biases, the VVDS-Deep survey has been conceived as a purely flux-limited ($17.5 \leq I \leq 24$) survey, i.e. no target pre-selection according to colors or compactness is used. Stars and QSOs have been a-posteriori removed from the final redshift sample. Photometric data in this field are complete and free from surface brightness selection effects, down to the limiting magnitude $I_{AB} = 24$ (Mc Cracken et al. 2003). Spectroscopic observations were carried out using the VIMOS multi-object spectrograph using one arcsecond wide slits and the LRRed grism which covers the spectral range $5500 < \lambda(\text{Å}) < 9400$ with an effective spectral resolution $R \sim 227$ at $\lambda = 7500$ Å. The rms accuracy in the redshift measurements is $\sim$275 km s^{-1}. Details on the observations and data reduction are given in Le Fèvre et al. (2004, 2005).

The VVDS-02h data sample extends over an area of 0.7×0.7 sq deg (which was targeted according to a one, two or four passes strategy, i.e. giving to any single galaxy in the field one, two or four chances to be targeted by VIMOS masks (see Fig. 12 in Le Fèvre et al. 2005) has a median depth of about $z \sim 0.76$. It contains 6582 galaxies with secure redshifts (i.e. redshift determined with a quality flag ≥ 2, see Le Fèvre et al. 2005) and probes a comoving volume (up to $z = 1.5$) of nearly $1.5 \times 10^6\ h^{-3}\,\text{Mpc}^3$. This volume has transverse dimensions $\sim 37 \times 37\ h^{-1}$ Mpc at $z = 1.5$ and extends over a comoving length of $3060\ h^{-1}$ Mpc in the radial direction.

For the statistical analysis presented in this paper, we first define a sub-sample (VVDS-02h-4) including galaxies with redshift $z < 1.5$ and over the sky region (0.4×0.4 deg^2) that was repeatedly covered by four independent VIMOS observations in each point. Even if measured redshifts in the VVDS reach up to $z \sim 5$ and cover a wider area, these conservative limits bracket the range where we can sample in a denser way the underlying galaxy distribution and, thus, minimise biases in the reconstruction of the density field (see the analysis in Sect. 4.1). The VVDS-02h-4 subsample contains 3448 galaxies with secure redshift (3001 with $0.4 < z < 1.5$), probes one-third of the total VVDS-02h volume and it is characterised by a redshift sampling rate of $\sim$30% (i.e. on average about one over three galaxies with magnitude $I_{AB} \leq 24$ has a measured redshift). This high spatial sampling rate is a critical factor for minimising biases in the reconstruction of the 3D density field of galaxies. To optimise the analysis of the associated probability density function, we further select only galaxies with absolute blue magnitude $M_B < -20 + \log h$. With this selection, we define two nearly volume-limited sub-samples in the redshift ranges $0.7 < z < 1.1$ and $1.1 < z < 1.5$ respectively. A discussion of possible effects of galaxy evolution on our results is presented in Sect. 4.3.

3. The galaxy density field at high redshift

The first large redshift surveys of the local Universe (e.g. Davis & Huchra 1981; Geller & Huchra 1991; Giovanelli & Haynes 1991; Strauss et al. 1992a; da Costa et al. 1994) showed that galaxies have a highly non-random spatial distribution and cluster in a hierarchical fashion. The corresponding three-dimensional maps reveal a complex web-like network of thin, filamentary structures connecting centrally condensed clusters of galaxies, punctuated by large, quasi-spherical, low-density voids. These structures are the outcome of more than 13 billion years of evolution of small-amplitude fluctuations that we see reflected in the temperature anisotropy of the Cosmic Microwave Background (CMB) at $z \simeq 1100$ (Spergel et al. 2007). Recent analyses (e.g. Tegmark et al. 2006) have shown the remarkable consistency between two-point statistics of the galaxy distribution at $z \sim 0$ and the CMB power spectrum which probes matter clustering at the recombination. Mapping the large-scale structure at $z \sim 1$ is thus crucial to further test the coherency of the gravitational instability picture at an intermediate time between the epoch of last scattering and today.

In this section we present a reconstruction of the 3D galaxy density field, discussing first the methodology and summarising the techniques adopted to correct for observational selection effects. These are fully presented in Marinoni et al. (2005, hereafter Paper I) and Cucciati et al. (2006), to which the reader is referred for more details.

3.1. Density reconstruction method

The continuous galaxy density fluctuation field

$$\delta_{\rm g}(\boldsymbol{r}, \boldsymbol{R}) = \frac{\rho(\boldsymbol{r}, R) - \bar{\rho}}{\bar{\rho}} \tag{1}$$

represents the adimensional excess/deficit of galaxies on a scale R, at any given comoving position $\boldsymbol{r}$ with respect to the mean density $\bar{\rho}$. As suggested by Strauss & Willick (1995) we estimate the smoothed number density of galaxies brighter than $\mathcal{M}_{\rm c}$ on a scale R, $\rho(r, R, <\mathcal{M}_{\rm c})$, by summing over an appropriately weighted convolution of Dirac-delta functions with a normalised Gaussian filter F

$$\rho(\boldsymbol{r}, R, <\mathcal{M}_{\rm c}) = \sum_i \frac{\int_0^\infty \delta^D(u - |\Delta \boldsymbol{r}_i|/R) F(u) {\rm d}u}{S(r_i, \mathcal{M}_{\rm c}) \Phi(m) \zeta(r_i, m) \Psi(\alpha, \delta)} \tag{2}$$

$$F(u) = \left(2\pi R^2\right)^{-3/2} \exp\left[-\frac{1}{2}u^2\right]. \tag{3}$$

Here $\Delta \boldsymbol{r} = (\boldsymbol{r}_i - \boldsymbol{r})$ is the separation between galaxy positions and the location $\boldsymbol{r}$ where the density field is evaluated. We compute the characteristic mean density at position $\boldsymbol{r}$ using Eq. (2) by simply averaging the galaxy distribution in survey slices $r \pm R_{\rm s}$, with $R_{\rm s} = 400\ h^{-1}$ Mpc. The four functions in the denominator of Eq. (2) correct for various observational characteristics:

- $S(r_i, \mathcal{M}_{\rm c})$ is the distance-dependent selection function of the sample. This function is identically one when a volume-limited sample is used. When the full magnitude-limited survey ($17.5 < I < 24$ in our case) is used, however, this function corrects for the progressive radial incompleteness due to the fact at any given redshift we can only observe galaxies in a varying absolute magnitude range. While the PDF of galaxy fluctuations will be derived from volume-limited samples, in the next section we shall make use of this function when reconstructing a minimum-variance 3D density map from the full VVDS survey.

The actual values of $S(r, \mathcal{M}_{\rm c})$ are derived using the VVDS galaxy luminosity function (Ilbert et al. 2005), assuming a minimum absolute magnitude $\mathcal{M}_{\rm c} = -15 + 5 \log h$ and accounting for its evolution as measured from the VVDS itself. A more detailed discussion of the derivation of the selection function can be found in Paper I

- $\Phi(m)$ corrects for the slight bias against bright objects introduced by the slit positioning tool VMMPS/SPOC (Bottini et al. 2005).
- $\zeta(r_i, m)$ is the correction for the varying spectroscopic success rate as a function of the apparent I_{AB} magnitude and of the distance of the object (see Ilbert et al. 2005).
- $\Psi(\alpha, \delta)$ is the angular selection function correcting for the uneven spectroscopic sampling of the VVDS on the sky (see Fig. 1, of Cucciati et al. 2006). Its purpose is to make allowance for the different number of passes done by the VIMOS spectrograph in different sky regions (a factor which is anyway maximised in the 4-pass sub-area of the sample).

The analytical form of these selection functions is discussed in Cucciati et al. (2006). The underlying assumption in this reconstruction scheme is that the subset of observed galaxies (e.g. in the case of a flux-limited sample, those luminous enough to enter the sample at a given redshift) is representative of the full population. This assumption clearly neglects any dependence of clustering on luminosity and could bias the density field reconstructed from the pure flux-limited sample at different redshifts; for this reason, the quantitative measurements presented in this paper will all be based on quasi-volume-limited samples, limited to an absolute magnitude $M_B = -20 + 5 \log h$. Finally, it should also be mentioned that in adopting a universal luminosity function we do not take into account the possible dependence of the luminosity function on morphological type and environment; this is, however, a second order effect in this work.

The shot-noise error affecting the reconstructed field at different $\boldsymbol{r}$ is estimated by computing the square root of the variance

$$\epsilon(\boldsymbol{r}) = \frac{1}{\overline{\rho_{\rm g}}} \left[\sum_i \left(\frac{F\left(\frac{|\Delta \boldsymbol{r}_i|}{R}\right)}{S(r_i, \mathcal{M}^{\rm c}) \Phi(m_i), \zeta(z, m), \Psi(\alpha, \delta)} \right)^2 \right]^{1/2}. \tag{4}$$

The amplitude of the shot noise increases as a function of redshift in a purely flux-limited survey. We deconvolve the signature of this noise from the density maps by applying the Wiener filter (cf. Press et al. 1992; Strauss et al. 1992b) which provides the *minimum variance* reconstruction of the smoothed density field, given the map of the noise and the a priori knowledge of the underlying power spectrum (e.g. Lahav et al. 1994). For this we assume that the observed galaxy density field $\delta_{\rm g}(\boldsymbol{r})$, and the true (i.e. including all galaxies) underlying field $\delta_{\rm T}(\boldsymbol{r})$, both smoothed on the same scale, are related via

$$\delta_{\rm g}(\boldsymbol{r}) = \delta_{\rm T}(\boldsymbol{r}) + \epsilon(\boldsymbol{r}), \tag{5}$$

where $\epsilon(\boldsymbol{r})$ is the local contribution from shot noise (see Eq. (4)). The Wiener filtered density field, in Fourier space, is

$$\tilde{\delta}_{\rm F}(\boldsymbol{k}) = \mathcal{F}(\boldsymbol{k}) \tilde{\delta}_{\rm g}(\boldsymbol{k}), \tag{6}$$

where

$$\mathcal{F}(\boldsymbol{k}) = \frac{\langle \tilde{\delta}^2_{\rm T}(\boldsymbol{k}) \rangle}{\langle \tilde{\delta}^2_{\rm T}(\boldsymbol{k}) \rangle + (2\pi)^3 P_\epsilon(\boldsymbol{k})}. \tag{7}$$

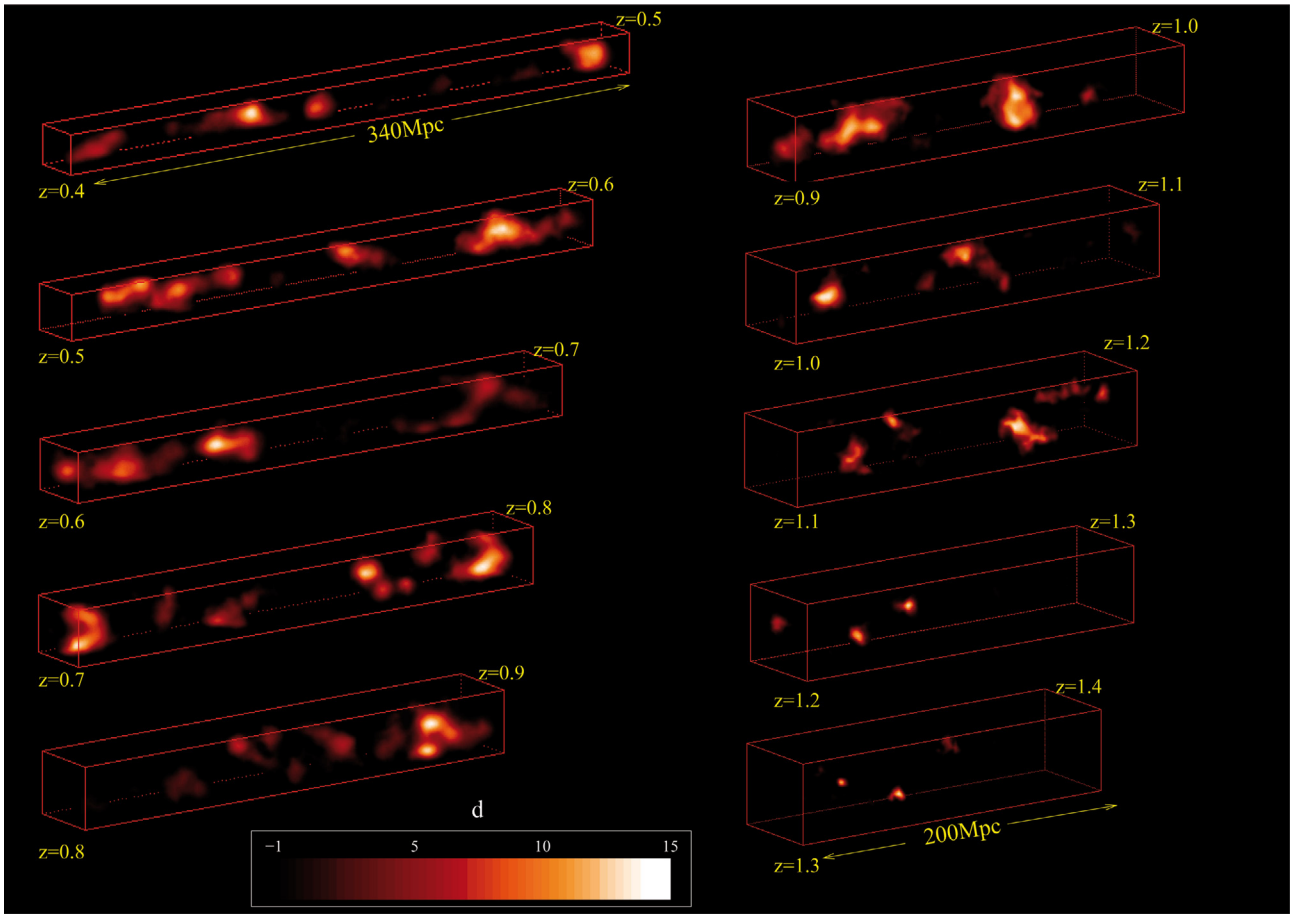

Fig. 1. The reconstructed density field for $0.4 < z < 1.4$, as traced by the galaxy distribution in the VVDS-Deep redshift survey to $I \leq 24$. This figure preserves the correct aspect ratio between transverse and radial dimensions. The mean inter-galaxy separation of this sample at the typical depth of the VVDS ($z = 0.75$) is 4.6 h^{-1} Mpc, comparable to local redshift surveys as the 2dFGRS. The galaxy density distribution has been smoothed using a 3D Gaussian window of radius $R = 2\ h^{-1}$ Mpc and noise has been filtered away using a Wiener filtering technique (see Strauss & Willick 1995; Marinoni et al. 2005). Only fluctuations above a signal-to-noise threshold of 2 are shown. The accuracy and robustness of the reconstruction methods have been tested using realistic mock catalogues (Pollo et al. 2005; Marinoni et al. 2005).

where brackets denote statistical averages and where $P_\epsilon(\boldsymbol{k}) = (2\pi)^{-3}\langle|\tilde{\epsilon}^2(\boldsymbol{k})|\rangle$ is the power spectrum of the noise. Assuming ergodic conditions, this last quantity can be computed as $P_\epsilon(\boldsymbol{k}) = (2\pi)^{-3}|\tilde{\epsilon}(\boldsymbol{k})|^2$. The calculation of $\langle\tilde{\delta}^2_{\rm T}(\boldsymbol{k})\rangle$ taking into account the form of the window function F and the peculiar VVDS survey geometry is presented in Paper I.

3.2. A cosmographical tour up to $z = 1.5$

We have first applied our reconstruction technique to the global flux-limited VVDS sample to build a visual three-dimensional map of galaxy density fluctuations to $z = 1.5$ which exploits the full information content of the survey. The $I \leq 24$ sample is characterised by an effective mean inter-particle separation of ($\langle r\rangle \sim 5.1\ h^{-1}$ Mpc) in the redshift range $[0, 1.5]$. For comparison, this sampling is better (denser) than the early CfA1 survey ($\langle r\rangle \sim 5.5\ h^{-1}$ Mpc) used by Davis & Huchra (1981) to reconstruct the 3D density field of the local Universe (i.e. out to $\sim$80 h^{-1} Mpc). Also, at the median depth of our survey, i.e. in the redshift interval $0.7 < z < 0.8$, the mean inter-particle separation is 4.4 h^{-1} Mpc, a value nearly equal to the 2dFGRS at its median depth.

The recovered galaxy density field is presented in Fig. 1. Fluctuations have been smoothed on a scale $R = 2\ h^{-1}$ Mpc. Only density contrasts with signal-to-noise ratio $S/N > 2$ are shown.

A remarkable feature of this "*geographical*" exploration of the Universe at early cosmic epochs is the abundance of large-scale structures similar in density contrast and size (at least in one direction) to those observed by local surveys. In particular, it is tempting to identify qualitatively a few filament-like density enhancements bridging more condensed structures along the line of sight, although the survey transverse size is still too small to fully sample their extent. Nevertheless, it is interesting to notice that these apparently one-dimensional structures remain coherent over scales $\sim$100 h^{-1} Mpc, separating low-density regions of similar size. Figures one and two visually confirm that the familiar web pattern observed in the local Universe is not a present-day transient phase of the galaxy spatial organisation but it is already well-defined at $\sim$1.5 when the Universe was $\sim$30% its present age (e.g. Le Fèvre et al. 1996; Gerke et al. 2005; Scoville et al. 2007). This implies that large-scale features of the galaxy distribution essentially reflects the long-wavelength modes of the initial power spectrum, in agreement with theoretical predictions of the CDM hierarchical scenario. Numerical simulations of large scale structure formation in fact show that the present-day web of filaments and walls is actually present when the universe was in embryonic form in the overdensity pattern of the initial fluctuations, with subsequent linear and non-linear

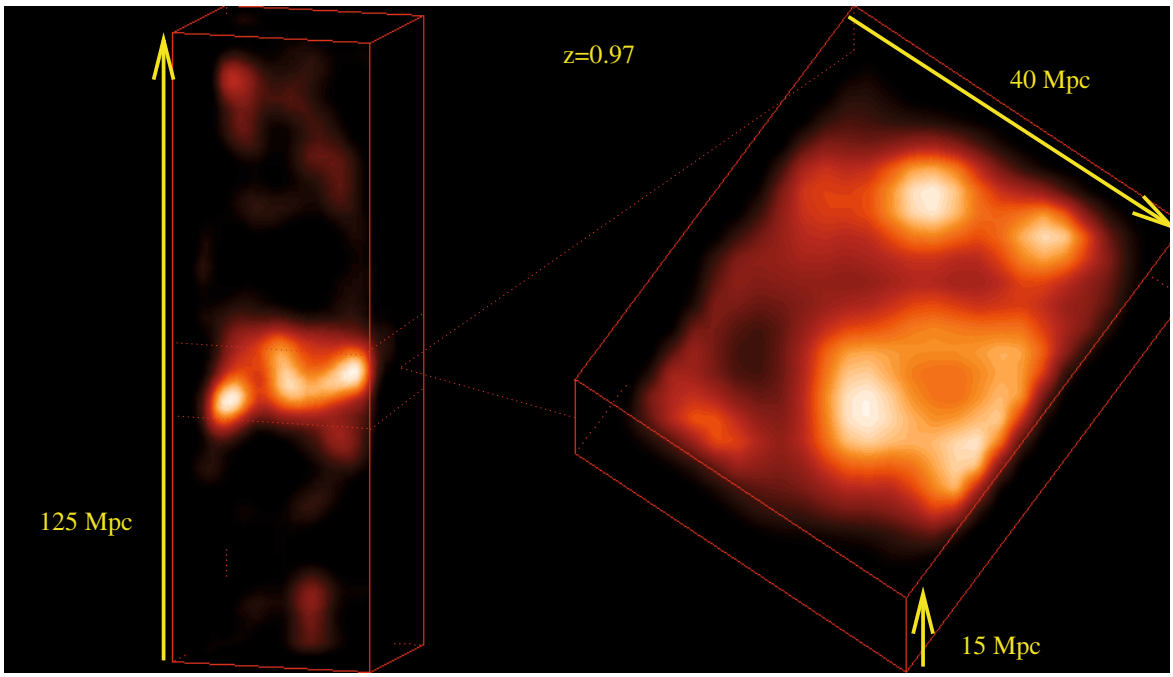

Fig. 2. Density distribution and properties of a large-scale planar structure at $z = 0.97$, that completely fills the VVDS-02h field-of-view.

gravitational dynamics just sharpening its features (e.g. Bond et al. 1996; Springel et al. 2005).

The limited angular size of the survey is exemplified by a dense "wall" at $z = 0.97$ that stretches across the whole survey solid angle (0.7×0.7 deg) (see Fig. 2). This two-dimensional structure is coherent over more than $\sim 30\ h^{-1}$ Mpc (comoving) in the transverse direction, is only $\sim 10\ h^{-1}$ Mpc thick along the line of sight, and has a mean overdensity $\delta_g = 2.4 \pm 0.3$. This makes it similar to the largest and rarest structures observed in the local Universe, such as the Shapley concentration (e.g. Scaramella et al. 1989; Bardelli et al. 2000). By applying a Voronoy-Delaunay cluster finding code (Marinoni et al. 2002), we find 10 distinct groups in this structure, with between 5 and 12 galaxy members each (down to the limiting magnitude $I = 24$), for a total of 164 galaxies. If one considers the evolution of *mass* fluctuations in the standard ΛCDM model, the probability of finding a structure with similar *mass* overdensity at such early times ($0.9 < z < 1$) would be nearly 4 times smaller than today: one such *mass fluctuation* would be expected in a volume of $\sim 3 \times 10^6\ h^{-3}$ Mpc^3, i.e. nearly 5 times larger than our surveyed volume up to $z \sim 1$. In fact, as we shall describe in Sect. 3.3, finding such a *galaxy* overdensity is not so unusual: it is clear evidence that the *biasing* between galaxies and matter at these epochs is higher than today. This makes fluctuations in the galaxy distribution to be highly enhanced with respect to those in the mass.

3.3. Evolution of the PDFs of galaxy fluctuations in the VVDS

Several approaches may be used to characterise in a quantitative way the distribution of galaxy fluctuations δ_g shown in Fig. 1. A complete specification of the overdensity field may be given by the full set of galaxy N-point correlation functions (Davis & Peebles 1977). This approach has been explored and routinely applied over the past decade as better and deeper redshift surveys have become available. An alternative description may instead be given in terms of the probability distribution function of a random field. By definition, the PDF of cosmological density fluctuations describes the probability of having a fluctuation in the range $(\delta, \delta + d\delta)$, within a spherical region of characteristic radius R randomly located in the survey volume. In principle, it encodes all the information contained within the full hierarchy of correlation functions, and provides insights about the time evolution of density fluctuations. This definition can be applied either to the distribution of galaxies, characterizing their number density fluctuations, or to the dark-matter dominated mass distribution. For the latter case, the expected shape of the PDF can be predicted as a function of redshift given a cosmological model, at least for large-scale fluctuations; this can be done either analytically (see below) or using numerical simulations.

On the observational side, in the case of surveys of the local Universe this fundamental statistics has been often overlooked (but see Marinoni & Hudson 2002; Ostriker et al. 2003). On the other hand, only recently deep redshift surveys have reached sufficient volumes to allow these measurements to be extended back in time. In Paper I, we have discussed and tested in detail the methodology to estimate the PDF from this kind of samples. In particular we have checked the robustness of the reconstruction against the specific VVDS-02h survey selection function, shot-noise errors and other observational biases. We used fully realistic mock samples of the VVDS-02h survey data and showed that, once the smoothing scale R is larger than the mean inter-galaxy separation, the overall shape of the reconstructed PDF is an unbiased realisation of the complete parent galaxy population. In particular, we showed that for redshifts up to $z = 1.5$ the VVDS-02h sky coverage and sampling rate are sufficient for obtaining a reliable reconstruction of the PDF shape (in both low- and high-density regions) on scales $R \geq 8\ h^{-1}$ Mpc. Clearly, the degree with which the PDF measured from this sample is a fair representation of the "universal" PDF up to $z = 1.5$ is a separate, yet critical question. A difference is naturally expected due to fluctuations on scales larger than the volume probed ("cosmic variance"). An estimate of this effect is actually included in our error bars, as these were drawn from the scatter among our set of VVDS mock samples.

We have therefore applied the estimator of Eq. (2) and the full de-noising technique described in Sect. 3.1 to the two luminosity-limited sub-samples of our survey described in Sect. 2, reconstructing the PDF of galaxy fluctuations in top-hat spheres of radius $R = 10\ h^{-1}$ Mpc at two different epochs ($0.7 < z < 1.1$ and $1.1 \leq z < 1.5$). The typical luminosity of the galaxies selected in these two intervals ($M_B \leq -20+5\log h$) corresponds to a median luminosity $L_B \simeq 2L_B^*$ at $z \sim 0$ (i.e. the same median luminosity of the whole 2dFGRS sample, Verde et al. 2002). As discussed previously, the use of luminosity-selected samples virtually eliminates distance-dependent shot-noise contributions (clearly neglecting the residual evolution within the two redshift bins, which is well within the errors). The results are shown in Fig. 3. The measured PDF's in Fig. 3 show several interesting features. First, as times passes (redshift decreases) the maximum of the PDF shifts to smaller δ-values; secondly, the low-density tail is enhanced, with more low-density regions appearing at lower redshifts. Quantitatively, this implies in particular that the probability of having an under-dense ($\delta_g < 0$) region of radius $R = 10\ h^{-1}$ Mpc at $0.7 \leq z < 1.1$ is nearly 10% larger than at earlier times ($1.1 \leq z < 1.5$).

3.4. The expected PDF of mass fluctuations in the mildly non-linear regime

The shape of the PDF of the galaxy overdensities is strongly dependent on the non-linear effects implicit both in the gravitational growth and in the physical mechanisms responsible for galaxy formation (e.g. Watts & Taylor 2000). Initial density fluctuations are normally assumed to have a Gaussian PDF; this is then modified by the action of gravity and, in the case of the galaxy field, by the way galaxies trace the underlying mass (*biasing* scheme). If galaxies were faithful and unbiased tracers of the underlying mass, the peak shift and the development of a low-density tail we observe in Fig. 3 could be naturally interpreted as the key signature of dynamical evolution purely driven by gravity. In fact, gravitational growth in an expanding Universe makes low density regions propagate outwards and become more common as time goes by, while at the same time the high-density tail increases.

If this interpretation is correct, we expect the PDF of galaxy overdensities to coincide with the PDF of mass fluctuations in each redshift range, once they are normalised to the observed clustering at $z \sim 0$, where we know that $L \sim 2\ L^*$ galaxies trace the mass (Verde et al. 2002). Let us verify whether this is the case by first summarising the main formalism to compute the PDF of mass fluctuations in a given cosmological scenario.

In hierarchical models, it is well established from numerical simulations that when structure growth reaches the nonlinear regime on a scale R, the PDF of mass density contrasts in comoving space is well described by a lognormal distribution (Coles & Jones 1991; Kofman et al. 1994; Taylor & Watts 2000; Kayo et al. 2001),

$$f_R(\delta) = \frac{(2\pi\omega_R^2)^{-1/2.}}{1+\delta} \exp\left\{-\frac{[\ln(1+\delta)+\omega_R^2/2]^2}{2\,\omega_R^2}\right\}. \quad (8)$$

This is fully characterised by a single parameter ω_R, related to the variance of the δ-field on a scale R as

$$\omega_R^2 = \ln[1+\langle\delta^2\rangle_R]. \quad (9)$$

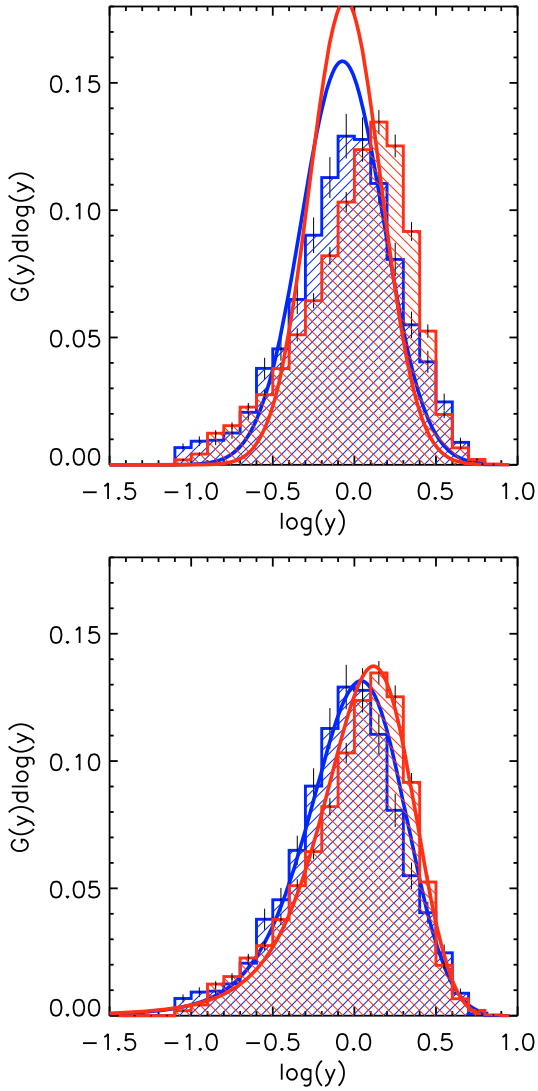

Fig. 3. The PDF of galaxy fluctuations (in units $y = 1+\delta$) for VVDS galaxies with $M_B \leq -20+5\log h$ from the VVDS within two independent volumes, corresponding to different cosmic epochs: $0.7 < z < 1.1$ (blue shaded histogram), and $1.1 \leq z < 1.5$ (green shaded histogram). The galaxy PDF has been reconstructed using a Top-Hat smoothing window of comoving size $R = 10\ h^{-1}$ Mpc. The histograms actually correspond to the distribution function $G(y) = \ln(10)yg(y)$ because the binning is done in $\log(y)$. The two observed histograms have been reproduced in both the upper and lower panels. They are compared to the theoretical predictions for the PDF of, respectively, mass fluctuations (*top*, from Eq. (8)) and of *galaxy* fluctuations as inferred from Eq. (14) using the non-linear biasing function measured from the VVDS (*bottom*). The blue and red lines correspond to the higher- and lower-redshift samples respectively.

At high redshifts, the variance $\sigma_R^2 \equiv \langle\delta^2\rangle_R$ over sufficiently large scales R (those explored in this paper) is given in the linear theory approximation by

$$\sigma_R(z) = \sigma_R(0)D(z) \quad (10)$$

where $D(z)$ is the linear growth factor of density fluctuations (normalised to unity at $z = 0$),

$$D(z) = \exp -\left[\int_0^z f(z)\,\mathrm{d}\ln(1+z)\right]. \quad (11)$$

In the standard ΛCDM cosmological model, the expression for the logarithmic derivative of the growth factor, $f = \mathrm{d}\log D/\mathrm{d}\log a$ (with $a = (1+z)^{-1}$), can be approximated to excellent accuracy as

$$f(z) \sim \Omega_{\rm m}^{\gamma}(z)$$

where $\gamma \simeq 0.55$ (Wang & Steinhardt 1998; Linder 2005) and

$$\Omega_{\rm m}(z) = \Omega_{\rm m}^{0}\frac{(1+z)^3}{E^2(z)}$$

$$E^2(z) = \Omega_{\rm m}^{0}(1+z)^3 + \Omega_{\Lambda}.$$

The lognormal approximation formally describes the distribution of matter fluctuations computed in real comoving coordinates. On the contrary, the PDF of galaxies is observationally derived in redshift space, where its shape is distorted by the effects of peculiar motions (e.g. Marinoni et al. 1998; Guzzo et al. 2008). In order to map properly the mass overdensities into galaxy overdensities the mass and galaxy PDFs must be computed in a common reference frame. It has been shown by Sigad et al. (2000) that an optimal strategy to derive galaxy biasing is to compare both mass and galaxy density fields directly in redshift space. Implicit in this approach is the assumption that mass and galaxies are statistically affected in the same way by gravitational perturbations, i.e. that there is no velocity bias in the motion of the two components.

The relation between the variances measured in real and redshift comoving space is

$$\sigma_R^z(z) = p(z)\sigma_R(z) \tag{12}$$

where $p(z)$ is a redshift-dependent correcting factor which takes into account the average contribution of the linear redshift distortions induced by peculiar velocities (Kaiser 1987). Its expression, in the high redshift regime, is given by (Hamilton 1998; Marinoni et al. 2005)

$$p(z) = \left[1 + \frac{2}{3}f(z) + \frac{1}{5}f^2(z)\right]^{1/2}. \tag{13}$$

We have used this formalism to compute the PDF expected for mass fluctuations in the redshift ranges explored using our galaxy samples. This is given, for the two ranges, by the curves in the top panel of Fig. 3. The evident discrepancy between the galaxy and mass PDF's indicates that the observed evolution cannot be only the product of gravitational growth (in the adopted cosmological model), but that a time-evolving bias between the galaxy and mass density fields is needed: at high redshifts and on large scales galaxy overdensities trace in a more biased way the underlying pattern of dark matter fluctuations. In the following section we shall summarise our current knowledge on the properties and evolution of the biasing function and show how the presence of a non-linear bias is a necessary ingredient to theoretically understand the evolution of the PDF in Fig. 3. This will in particular provide us with the necessary background to interpret the evolution of the low-order moments of the PDF at different redshifts, which is our aim in this paper.

3.5. Evolution and non-linearity of biasing

Biasing lies at the heart of all interpretations of large-scale structure models. Structure formation theories predict the distribution of mass; thus, the role of biasing is pivotal in mapping the observed light distribution back into the theoretical model. In our case we need to disentangle the imprint of biasing from that of pure gravity in the evolution of the galaxy PDF.

In Paper I we inferred the biasing relation $\delta_{\rm g} = \delta_{\rm g}(\delta) = b(\delta)\delta$ between mass and galaxy overdensities from their respective probability distribution functions $f(\delta)$ and $g(\delta_{\rm g})$. Assuming a one-to-one mapping between mass and galaxy overdensity fields, conservation of probabilities implies (e.g. Sigad et al. 2000; Wild et al. 2005)

$$g(\delta_{\rm g})\mathrm{d}\delta_{\rm g} = f(\delta)\mathrm{d}\delta. \tag{14}$$

This approach implies the assumption of a cosmological model (the standard ΛCDM model in our case) from which to compute $f(\delta)$, the mass PDF. The advantage over other methods is that we can explore the functional form of the relationship $\delta_{\rm g} = b(z,\delta,R)\delta$ over a wide range in mass density contrasts, redshift intervals and smoothing scales R without imposing any a-priori parametric functional form for the biasing function. Note that, by definition, this scheme is ineffective in capturing information about possible stochastic properties of the biasing function.

The numerical solution $\delta_{\rm g} = \delta_{\rm g}(\delta)$ of Eq. (14) maps the mass PDF (solid lines in the top panel of Fig. 3) into the galaxy PDF (solid lines in the bottom panel of Fig. 3) and can be analytically approximated using a Taylor expansion (Fry & Gaztañaga 1993)

$$\delta_{\rm g}(\delta) = \sum_{k=0}^{n}\frac{b_k(z)}{k!}\delta^k, \tag{15}$$

where the coefficients b_i depend on redshift. We consider this power series only to second order, and fit the numerical solution for the biasing function leaving b_0 as a free parameter. Avoiding setting b_0 as an integral constraint ($\langle\delta_{\rm g}\rangle = 0$) allows us to account for possible (un-modelled) contributions from higher order moments of the expansion. This approach has the advantage of minimising biases in the estimates of the lower moments of the expansion, specifically b_1 and b_2.

The key result from Paper I has been to show that galaxy biasing is poorly described in terms of a single scalar and better characterised by a more sophisticated representation. Specifically, always considering a scale $R = 10\ h^{-1}$ Mpc, the ratio between the quadratic and linear bias terms has been evaluated in four different high redshift intervals (see Table 2 of Paper I). When averaged over the full redshift baseline $0.7 < z < 1.5$, this ratio turns out to be

$$\left\langle\frac{b_2}{b_1}\right\rangle = -0.19 \pm 0.04 \tag{16}$$

i.e. different from zero at more than 4σ confidence level. This means that – at least over the redshift range and scales considered here – the level of biasing depends on the underlying value of the mass density field. In other words, the way galaxies are distributed in space depends in a non-linear manner on the local amplitude of dark matter fluctuations.

The measurement of a non-linear term in the biasing relation is fully consistent with a parallel analysis of the hierarchical scaling of the N-point correlation functions in the same VVDS sample (Cappi et al. 2008). These results confirm a generic prediction of hierarchical models of galaxy formation (e.g. Somerville et al. 2001). It is relevant to compare them to estimates of the bias function at the current epoch. Early works indirectly suggested that also at $z \sim 0$ the biasing function should have a non-negligible non-linear component. Comparing the two-point correlation functions and the normalized skewness of SSRS2

galaxies, Benoist et al. (1999) showed that the relative bias between galaxies with different luminosity is non-linear, which indirectly indicates that (at least for luminous galaxies) the bias with respect to the dark matter must be non-linear as well. A similar analysis was performed by Baugh et al. (2004) and Croton et al. (2004) on the 2dFGRS, finding results consistent with Benoist et al.; finally, Feldman et al. (2001) and Gaztañaga et al. (2005) directly measured the three-point correlation function (in both Fourier and real space) for the IRAS and 2dFGRS samples respectively and found evidence for $b_2 < 0$.

On the other hand, these results seem to be inconsistent with another analysis of the 2dFGRS performed using the bispectrum (Verde et al. 2002). Hikage et al. (2005) by analysing the SDSS galaxies with a Fourier-phase technique also conclude that the bias in this survey is essentially linear. If one ignored the other independent analysis of the 2dFGRS, it could be speculated that the large-scale non-linear term that we detect at $z > 0.7$ is suppressed as a function of cosmic time; this is however not supported by the results of numerical experiments (Somerville et al. 2001). Interestingly, we note that when compared to the local non-linear measurements ($b_2/b_1 \sim -0.35$) (Feldman et al. 2001; Gaztañaga et al. 2005), our estimate seems to suggest that the amplitude of the quadratic term b_2/b_1 decreases (in absolute terms) as a function of redshift, a results in qualitative agreement with indications from simulations. It seems therefore more likely that the difference in the reconstruction methods used (with different sensitivity to higher order terms in Eq. (15)) is a better explanation of the discrepant results at $z \sim 0$. We will show in the next section (Sect. 4) how the self-consistency of the evolution of the variance and skewness of galaxy counts with redshift, indeed requires the presence of a non-linear biasing component.

The information contained in the non-linear function of Eq. (15) can be compressed into a single scalar term that can be used to interpret the evolution of two-point statistics (correlation function) as well as the variance of the galaxy density field (see Sect. 4.2). Since, by definition, $\langle b(\delta)\delta\rangle = 0$, the most interesting linear bias estimators are associated to the second order moments of the PDFs, i.e. the variance $\langle\delta_{\rm g}^2\rangle$ and the covariance $\langle\delta_{\rm g}\,\delta\rangle$. Following the prescriptions of Dekel & Lahav (1999), we characterize the biasing function as follows

$$b_{\rm L}^2 \equiv \frac{\langle b^2(\delta)\,\delta^2\rangle}{\langle\delta^2\rangle} \tag{17}$$

where $b_{\rm L}^2$ is an estimator of the linear biasing parameter defined, in terms of the two-point correlation function, as $\xi_{\rm g} = b_{\rm L}^2\xi$. We evaluate Eq. (17) using Eq. (15) with parameters $b_i(z)$ estimated locally by Verde et al. (2002) and in the redshift range $0.4 < z < 1.5$ by Marinoni et al. (2005). The best fitting phenomenological model describing the redshift scaling of the linear biasing parameter for a volume limited population of "normal" galaxies with median luminosity $L \sim 2L^*(z = 0)$ is

$$b_{\rm L}(z) = 1 + (0.03 \pm 0.01)(1+z)^{3.3\pm0.6}.$$

While today $\sim 2L^*$ galaxies trace the underlying mass distribution on large scales (Lahav et al. 2002; Verde et al. 2002; Gaztañaga et al. 2005), in the past the two fields were progressively dissimilar and the relative biasing systematically higher. In Paper I we showed how this observed redshift trend compares to different theoretical models for biasing evolution, i.e. a "galaxy conserving" model (Fry et al. 1996), a "halo merging" model (Mo & White 1996) and a "star forming" model (Tegmark & Peebles 1998).

4. Testing gravitational instability with the low-order moments of the PDF

Having decoupled biasing effects from the purely gravitational evolution of the galaxy PDF we have now all the ingredients to use this latter quantity to test the consistency of some general predictions of the GIP. The evolution of the low-order statistical moments of the galaxy PDF, specifically its second and third moments can be compared, on large scales with analytical predictions of linear and second order perturbation theory respectively.

4.1. Estimating the moments from redshift survey data

Following standard conventions, we define the second- and third-order moments, on a scale R, of a continuous, zero-mean overdensity field as

$$\langle\delta_{\rm g}^2\rangle_R = \int_{-1}^{\infty}\delta_{\rm g}^2 g_R(\delta_{\rm g})\mathrm{d}\delta_{\rm g}, \tag{18}$$

and

$$\langle\delta_{\rm g}^3\rangle_R = \int_{-1}^{\infty}\delta_{\rm g}^3 g_R(\delta_{\rm g})\mathrm{d}\delta_{\rm g}. \tag{19}$$

Note that the moments cannot be estimated as ensemble averages over the reconstructed PDF. In fact, this last quantity has been reconstructed using the Wiener filtering technique. This minimises the shot noise contribution (Sect. 3.1) but gives a biased estimate of the density field moments (via Eqs. (18) and (19)) as it requires an input power spectrum (and therefore *assuming* a second moment). A standard practical way to estimate moments is to randomly throw spherical cells down within the galaxy distribution and reconstruct the count probability distribution function $P_k = n_k/N$ (where n_k is the number of cells that contain k galaxies out of a total number of cells N. The moments are then estimated as

$$\langle\delta_{\rm g}^p\rangle = \bar{N}^{-p}\sum_{k=0}^{\infty}P_k\langle(k-\bar{N})^p\rangle \tag{20}$$

where $\bar{N} = \sum_{k=0}^{\infty}kP_k$.

The quantities we are interested in are the cumulants $\langle\delta^p\rangle_{\rm c}$ of the one-point density PDF. For a density field smoothed with a top-hat window, the p-order cumulant

$$\langle\delta_{\rm g}^p\rangle_{\rm c} = \frac{1}{v_R^p}\int\xi_p(r_1, r_2...r_p)\mathrm{d}^3r_1\mathrm{d}^3r_2...\mathrm{d}^3r_p \tag{21}$$

is the average of the N-point reduced correlation function over the corresponding cell of volume v_R (from now on we will only consider the scale $R = 10\,h^{-1}$ Mpc and we will drop the suffix R, unless we need to emphasize it). This is defined as the connected part of the N-point correlation function $\langle\delta_{\rm g}(r_1)\delta_{\rm g}(r_2)...\delta_{\rm g}(r_p)\rangle$ in such a way that for $p > 2$ $\xi_p = 0$ for a Gaussian field. Since the galaxy distribution is a discrete process (Eq. (2) is a sum over Dirac delta functions) and since, by definition, the density contrast has a zero mean, the connection between low-order cumulants and moments is given by

$$\langle\delta_{\rm g}^2\rangle_{\rm c} = \langle\delta_{\rm g}^2\rangle - \frac{1}{\bar{N}} \tag{22}$$

$$\langle\delta_{\rm g}^3\rangle_{\rm c} = \langle\delta_{\rm g}^3\rangle - 3\frac{\langle\delta_{\rm g}^2\rangle_{\rm c}}{\bar{N}} - \frac{1}{\bar{N}^2}\,. \tag{23}$$

These relations accounts for discreteness effects using the Poisson shot-noise model (e.g. Peebles 1980; Fry 1985). Possible biases introduced by this technique are discussed by Hui & Gaztañaga 1999, while an alternative approach is detailed by Kim & Strauss (1998).

Finally, it is necessary to devise a strategy to compensate for the fact that a cell will sample regions that have varying angular and spectroscopic completeness and which may even span the survey boundary. For this reason the galaxy counts are scaled up in proportion to the degree of incompleteness in the cell. This is done by weighting galaxy counts using the selection functions $\Phi(m)$, $\zeta(r, m)$, and $\Psi(\alpha, \delta)$ defined in Sect. 3.1. Additionally, although our reconstruction scheme accounts for the non-uniform VVDS angular coverage, we further restrict ourselves to counts in spheres having at least 70% of their volume in the denser 4-pass region, in order to avoid possible edge effects. We remark that moments are estimated from virtually volume-limited samples, as defined in Sect. 2. As a consequence, the radial selection function is constant and any variations in the density of galaxies are due only to large-scale structure.

4.2. The evolution of the *rms* and skewness of galaxy fluctuations

Since in perturbation theory higher order cumulants are predicted to be a function of the variance, it is useful, in the following, to define the normalized skewness

$$S_3 = \langle \delta_g^3 \rangle_c / \sigma^4, \tag{24}$$

where the shot-noise corrected variance σ^2 is given by Eq. (22). Figure 4 shows the evolution of the rms fluctuation and the normalized skewness on a scale $R = 10\,h^{-1}$ Mpc, as measured from the VVDS volume-limited sub-samples. Errors have been computed using the 50 fully-realistic mock catalogs of VVDS-Deep discussed in Pollo et al. (2005). This allows us to include an estimate of the contribution of cosmic variance, which represents the most significant term in our error budget.

The top panel of Fig. 4 shows that the square-root of the variance, which measures the rms amplitude of fluctuations in galaxy counts, is with good approximation constant over the full redshift baseline investigated: in redshift space, the mean value of σ_g for our volume-limited galaxy samples is 0.78 ± 0.09 for $0.7 < z < 1.5$. A similar, nearly constant value is also consistent with the value estimated at $z \sim 0.15$ from the 2dF galaxy redshift survey (Croton et al. 2004) that is also reported in same figure. This means that over nearly 2/3 of the age of the Universe the observed fluctuations in the galaxy distribution look almost as frozen, despite the underlying gravitational growth of mass fluctuations. This quantifies the visual impression we had from Fig. 1, that the distribution of galaxies is as inhomogeneous at $z \sim 1$ as it is today.

The third moment, which measures asymmetries between under- and over-dense regions, indicates that the galaxy density field was non-Gaussian on large scales ($10\,h^{-1}$ Mpc) even at these remote epochs ($\sim 4\sigma$ detection). In particular we find indication for an increase of the normalised skewness with cosmic time, when comparing the VVDS values to the local measurement by 2dFGRS.

Using the measured bias evolution, we can translate the specific predictions of the GIP for the variance and skewness of the matter density field into the corresponding observed quantities.

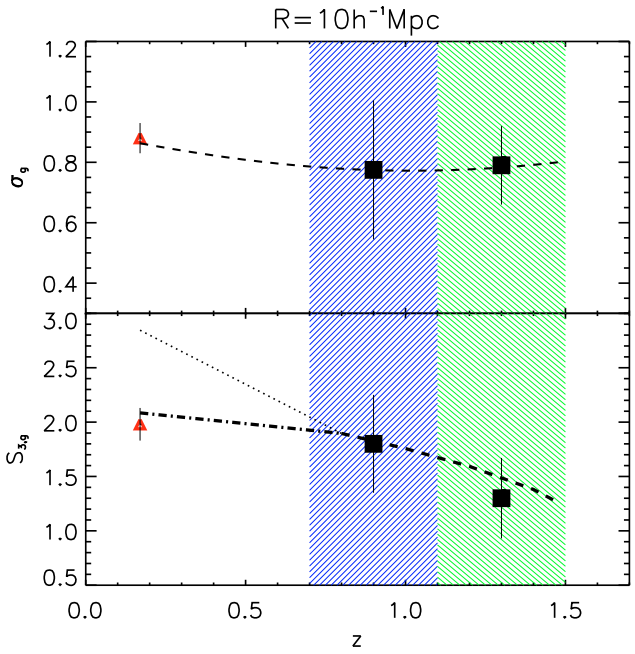

Fig. 4. Evolution of the rms deviation (*top*) and skewness (*bottom*) of the PDF of galaxy fluctuations on a scale $R = 10\,h^{-1}$ Mpc. The filled squares correspond to two volume-limited samples from the VVDS with $M_B < -20 + 5 \log h$ covering the redshift intervals indicated by the shaded regions. Triangles correspond to the 2dFGRS measurements at $z \simeq 0.15$ (Croton et al. 2004), from a sample including similarly bright galaxies. Error bars give 68% confidence errors, and, in the case of VVDS measurements, include the contribution from cosmic variance. The dashed lines in both panels show the theoretical predictions for the evolution of the variance (Eq. (25)) and skewness (Eq. (27)) inferred using VVDS measurement of biasing. Predictions for the skewness (based on the $(b_1(z), b_2(z))$ measurements in the redshift range $0.7 < z < 1.5$ quoted in Table 2 of Paper I) have been extrapolated to $z \sim 0$ using the local (2dFGRS) biasing measurements of Verde et al. (2002) (linear bias, dotted line) and of Gaztañaga et al. (2005) (quadratic bias with $b_2/b_1 = -0.34$, dot-dashed line).

Using linear perturbation theory, the scaling of the rms of number density fluctuations is

$$\sigma_g(z) \sim b_L(z) D(z) p(z) \sigma(0). \tag{25}$$

In a Universe in which primordial density fluctuations were Gaussian, the non-linear nature of gravitational dynamics leads to the emergence of a non-trivial skewness of the local density PDF.

Within the framework of gravitational perturbation theory, the first non-vanishing term describing the evolution of the skewness of a top-hat filtered, initially Gaussian matter density field corresponds to second-order.

According to non-linear, second-order perturbation theory predictions, the skewness of the mass distribution is approximately independent of time, scale, density, or geometry of the cosmological model. Assuming that its evolution only depends on the hypothesis that the initial fluctuations are small and quasi-Gaussian and that they grow via gravitational clustering one derives that, in redshift-distorted space (Peebles 1980; Juszkiewicz et al. 1993; Bernardeau 1994; Hivon et al. 1995)

$$S_3 \sim \frac{35.2}{7} - 1.15(n+3) \tag{26}$$

where n is the effective slope of the power spectrum on the scales of interest (i.e. in our case, since $R = 10\,h^{-1}$ Mpc , n is approximately given by -1.2, Bernardeau et al. e.g. 2002). Subsituting

the evolution of bias in second order approximation, the evolution of the observed skewness is given by (Fry & Gaztañaga 1993)

$$S_{3,g} \sim b_1(z)^{-1}\left[S_3 + 3\frac{b_2(z)}{b_1(z)}\right]. \quad (27)$$

The curves in both panels of Fig. 4 show that Eqs. (25) and (27) reproduce extremely well the evolution of variance and skewness observed within the VVDS.

The mass PDF is a one-parameter family of curves completely specified once the linear evolution model for the mass variance $\langle\delta^2\rangle$ is supplied. This implies that our *non-linear* biasing estimate is fully independent from predictions of higher-order perturbation theory. On the contrary, non-linear biasing at $z = 0$ is inferred by directly matching 3-point galaxy statistics with the corresponding mass statistics derived from weakly non-linear perturbation theory (e.g. Verde et al. 2000; Gaztañaga et al. 2005). As a consequence, the agreement we find between predicted and observed third-order moments is not a straightforward consequence of the method used to derive the biasing function. These results provide an indication of the consistency, at $z = 1$, of some constitutive elements of the standard picture of gravitational instability from Gaussian initial conditions.

Concerning the local measurements from 2dFGRS, the predicted scaling for the skewness continues to show very good agreement if the local, non-linear measurement of Gaztañaga et al. (2005) is considered. The value of $S_{3,g}$, however, cannot be consistent with GIP predictions if in the local universe the simple linear biasing measurement of Verde et al. (2002) (i.e. $b_2 = 0$) is adopted.

4.3. Effect of galaxy luminosity evolution

In the above comparison of galaxy samples at three different epochs, we have so far neglected an important point. Galaxy luminosity evolves significantly between $z \sim 0$ and $z \sim 1$, with a mean brightening of at least 1 magnitude for an average spectral type (Ilbert et al. 2005). Thus, the contribution to the clustering signal at progressively earlier epochs may not be be due to the progenitors of the galaxies that are sampled at later times in the same luminosity interval. Luminosity evolution between $z = 1$ and $z = 1.5$ is more uncertain but certainly smaller due to the shorter time interval. The brightening between the two VVDS sub-samples considered is expected not to be very significant for these very luminous objects.

To compare galaxies at $z = 1$ and $z \sim 0$ one should in principle confront our high-redshift results with those of local galaxies about one magnitude fainter. According to 2dFGRS results, this means shifting the local estimates of variance to a slightly smaller value (Norberg et al. 2002) and leaving the skewness measurement unchanged within the quoted error bars (Croton et al. 2004). These changes would only reinforce our conclusions about the evolution of the low order moments of the PDF of galaxy fluctuations. In particular, since a fainter sample has a smaller bias threshold, the locally measured skewness would make the discrepancy with GIP predictions for a simple linear biasing model even stronger.

5. Conclusions

The results presented in this paper provide the first direct evidence at $z \sim 1$ for the consistency of the GIP hypothesis as described in the framework of general relativity. The standard theory of structure formation via gravitational instability successfully explains the present day statistics (e.g. Tegmark et al. 2006) and dynamics (e.g. Peacock et al. 2001) of large scale structures. We have shown that observations are fully consistent with these predictions over the entire redshift baseline $0 < z < 1.5$ once the biasing between the galaxy and matter distribution is properly described. In Paper I we showed that it is necessary to include a small (10%) yet crucial non-linear component to accurately account for the observed probability distribution function of galaxy overdensities. Here we have shown that this component is also necessary as to understand the observed evolution of the low-order moments of the galaxy overdensity field.

More specifically, our analysis of the 3D density fluctuation field traced by a volume-limited sample of VVDS galaxies (with $M_B \leq -20 + 5\log h$) at different epochs unambiguously reveals the time-dependent effects of gravitational evolution:

a) Underdense regions progressively occupy a larger volume fraction as a function of cosmic time, as expected from gravitational growth in an expanding background.
b) The second moment of the field traced by this "normal" population of galaxies (with median luminosity $\sim 2\ L*$) is statistically consistent with the local ($z \sim 0$) estimate for similarly luminous galaxies, i.e. it is approximately constant over the full redshift baseline $0 < z < 1.5$. This implies that the apparent inhomogeneity in the galaxy distribution remains similar, i.e. galactic fluctuations have almost frozen over nearly 2/3 of the age of the universe (Giavalisco et al. 1998; Coil et al. 2004; Pollo et al. 2005). We have shown that this is readily explained by the combination of the gravitational growth of mass fluctuations with the evolution of the bias between galaxies and mass. These two factors almost cancel each other out.
c) There are some hints that the skewness increases with cosmic time, its value at $z \sim 1.5$ being nearly 2σ times lower than that measured locally by the 2dFGRS for similarly luminous galaxies. In particular, the measured value of the skewness at $z \sim 1.5$ (on scales $R = 10\ h^{-1}$ Mpc) indicates that galaxy fluctuations are strongly non-Gaussian ($\sim 4\sigma$ detection) even at such an early epoch (see Cappi et al. 2008, for a different approach which arrives at similar conclusions).
d) Remarkably, once VVDS measurements of non-linear biasing are included, both these trends are consistent with predictions of linear and second-order perturbation theory for the evolution of gravitational perturbations as described within the framework of general relativity.
e) We have shown that the values of the skewness we measure at high redshift are difficult to reconcile with the 2dFGRS measurements if local biasing is linear (Verde et al. 2002). A fully coherent gravitational picture emerges, however, over the whole baseline $0 < z < 1.5$ if the non-linearity of the local biasing function is taken into account, at the level estimated by Feldman et al. (2001) and Gaztañaga et al. (2005). Compared to these local measurements our results seem to suggest that the amplitude of the quadratic term $|b_2/b_1|$ is a decreasing function of redshift at least up to $z \sim 1.5$.

Acknowledgements. We thank the referee, M. Strauss, for important suggestions that significantly improved the manuscript. L.G. acknowledges the hospitality of MPE and the "Excellence Cluster Universe" in Garching, where part of this work was completed. This research has been developed within the framework of the VVDS consortium and it has been partially supported by the CNRS-INSU and its Programme National de Cosmologie (France), and by the Italian Ministry (MIUR) grants COFIN2000 (MM02037133) and COFIN2003 (No. 2003020150). The VLT-VIMOS observations have been carried out on guaranteed time (GTO) allocated by the European Southern

Observatory (ESO) to the VIRMOS consortium, under a contractual agreement between the Centre National de la Recherche Scientifique of France, heading a consortium of French and Italian institutes, and ESO, to design, manufacture and test the VIMOS instrument.

References

Bardelli, S., Zucca, E., Zamorani, G., Moscardini, L., & Scaramella, R. 2000, MNRAS, 312, 540
Baugh, C. M., Croton, D. J., Gaztan aga, E., et al. 2004, MNRAS, 351, L44
Benoist, C., Cappi, A., da Costa, L. N., et al. 1999, ApJ, 514, 563
Bernardeau, F. 1994, ApJ, 433, 1
Bernardeau, F., Colombi S., Gaztañaga, E., & Scoccimarro, R. 2002, Phys. Rep., 367, 1
Bond, J. R., Kofman, L., & Pogosyan, D., 1996, Nature, 380, 603
Bouchet, F. R., Colombi, S., Hivon, E., & Juszkiewicz, R. 1995, A&A, 296, 575
Cappi, A., et al. (the VVDS team) 2008, in preparation
Coil, A. F., Davis, M., Madgwick, D. S., et al. 2004, ApJ, 609, 525
Coles, P., & Jones, B. 1991, MNRAS, 248, 1
Croton, D. J., Gaztan aga, E., Baugh, C. M., et al. 2004, MNRAS, 352, 1232
Cucciati, O., et al. (the VVDS team) 2006, A&A, 458, 39
da Costa, L. N., Geller, M. J., Pellegrini, P. S., et al. 1994, ApJ, 424, L1
Davis, M., & Peebles, P. J. E. 1977, ApJS, 34, 425
Davis, M., & Huchra, J. 1981, ApJ, 254, 437
Davis, M., et al. (the DEEP2 team) 2003, Proc. SPIE, 4834, 161
Dekel, A., & Lahav, O. 1999, ApJ, 520, 24
Feldman, H. A., Frieman, J. A., Fry, J. N., Scoccimarro, R. 2001, Phys. Rev. Lett., 86, 1434
Fry, J. N. 1985, ApJ, 289, 10
Fry, J. N., & Gaztañaga, E. 1993, ApJ, 413, 447
Gaztañaga, E., Norberg, P., Baugh, C. M., & Croton, D. J. 2005, MNRAS, 364, 620
Geller, M. J., & Huchra, J. P. 1989, Science, 246, 897
Gerke, B. F., Newman, J. A., Davis, M., et al. 2005, ApJ, 625, 6
Giavalisco, M., Steidel, C. C., Adelberger, K. L., et al. 1998, ApJ, 503, 543
Giovanelli, R., & Haynes, M. 1991, ARA&A, 29, 499
Guzzo, L., et al. (the VVDS team) 2008, Nature, 451, 541
Hamilton, A. J. S. 1998, in The Evolving Universe (Kluwer Astrophysics and Space Science Library), 185, 231, also [arXiv:astro-ph/9708102]
Hivon, R., Bouchet, F. R., Colombi, S., & Juszkiewicz, R. 1995, A&A, 298, 643
Hui, L., Gaztañaga, E. 1999, ApJ, 519, 622
Ilbert, O., et al. (the VVDS team) 2005, A&A, 439, 863
Juszkiewicz, R., Bouchet, F. R., & Colombi, S. 1993, ApJ, 412, L9 (34)
Kaiser, N. 1984, ApJ, 284, L9
Kaiser, N. 1987, MNRAS, 227, 1
Kayo, I., Taruya, A., & Suto, Y. 2001, ApJ, 561, 22
Kim, R. S., & Strauss, M. A. 1998, ApJ, 493, 39
Kofman, L., Bertshinger, E., Gelb, J. M., Nusser, A., & Dekel, A. 1994, ApJ, 420, 44
Lahav, O., Fisher, K. B., Hoffman, Y., Scharf, C. A., & Zaroubi, S. 1994, ApJ, 423, L93
Lahav, O., et al. 2002, MNRAS, 333, 961
Le Fèvre, O., et al. 1996, ApJ, 461, 534
Le Fèvre, O., et al. (the VVDS team) 2004, A&A, 428, 1043
Le Fèvre, O., et al. (the VVDS team) 2005, A&A, 439, 845
Lilly, S., et al. (the zCOSMOS team) 2007, ApJS, 172, 70
Linder, E. V. 2005, Ph. Rv. D, 72, 3529
Linder, E. V. 2007 [arXiv:0709.1113]
Marinoni, C., & Hudson, M. 2002, ApJ, 569, 101
Marinoni, C., Monaco, P., Giuricin, G., & Costantini, B. 1998, ApJ, 505, 484
Marinoni, C., Davis, M., Newmann, J. A., & Coil, A. L. 2002, ApJ, 580, 122
Marinoni, C., et al. (the VVDS team) 2005, A&A, 442, 801 (Paper I)
Massey, R., Rhodes, J., Ellis, R., et al. 2007, Nature, 445, 286
McCracken, H. J., Radovich, M., Bertin, E., et al. 2003, A&A, 410, 17
Oke, J. B., & Gunn, J. E. 1983, ApJ, 266, 713
Ostriker, J. P., Nagamine, K., Cen, R., & Fukugita, M. 2003, ApJ, 597, 1
Peacock, J. A., Cole, S., Norberg, P., et al. 2001, Nature, 410, 169
Peebles, P. J. E. 1980, The Large Scale Structure of the Universe (Princeton: Princeton Univ Press)
Pollo, A., et al. (the VVDS team) 2005, A&A, 439, 887
Pollo, A., et al. (the VVDS team) 2006, A&A, 451, 409
Press, W. H., Teukolsky, S. A., Vetterling, W. T., & Flannery, B. P. 1992, Numerical Recipes (Cambridge: University Press)
Scaramella, R., Baiesi-Pillastrini, G., Chincarini, G., Vettolani, G., & Zamorani, G. 1989, Nature, 338, 562
Scherrer, R. J., & Gaztanaga, E. 2001, MNRAS, 328, 257
Scoville, N. 2007, ApJS, 172, 150
Sigad, Y., Branchini, E., & Dekel, A. 2000, ApJ, 540, 62
Somerville, R. S., Lemson, G., Sigad, Y., et al. 2001, MNRAS, 320, 289
Spergel, D. N., Bean, R., Doré, O., et al. 2007, ApJS, 170, 377
Springel, W., White, S. D. M., Jenkins, A., et al. 2005, Nature, 435, 629
Strauss, M. A., et al. 1992, ApJS, 83, 29S
Strauss, M. A., & Willick, J. A. 1995, PhR, 261, 271
Strauss, M. A., Davis, M., Yahil, A., & Huchra, J. P. 1992, ApJ, 385, 421
Taylor, A. N., & Watts, P. I. R. 2000, MNRAS, 314, 92
Tegmark, M., et al. 2006, Phys. Rev. D, 74, 123507
Watts, P. I. R., Taylor, A. N. 2001, MNRAS, 320, 139
Verde, L., Heavens, A. F., Percival, W. J., et al. 2002, MNRAS, 335, 432
Wang, L., & Steinhardt, P. J. 1998, ApJ, 508, 483
Wild, V., Peacock, J. A., Lahav, O., et al. 2005, MNRAS, 356, 247